# Investigating generalized minimal supergravity in the MSSM through the long-lived bino NLSP at the HL-LHC

Wenxing Zhang,[1,2,3,4,*] Waqas Ahmed,[5,†] Imtiaz Khan,[6,7,‡] Tianjun Li,[6,7,§] and Shabbar Raza[8,‖]

[1]*Department of Physics, Hebei University, Baoding, 071002, China*
[2]*Hebei Key Laboratory of High-Precision Computation and Application of Quantum Field Theory, Baoding 071002, China*
[3]*Hebei Research Center of the Basic Discipline for Computational Physics, Baoding 071002, China*
[4]*Tsung-Dao Lee Institute and School of Physics and Astronomy, Shanghai Jiao Tong University, 800 Dongchuan Road, Shanghai 200240, China*
[5]*Center for Fundamental Physics and School of Mathematics and Physics, Hubei Polytechnic University, Huangshi 435003, China*
[6]*CAS Key Laboratory of Theoretical Physics, Institute of Theoretical Physics, Chinese Academy of Sciences, Beijing 100190, China*
[7]*School of Physical Sciences, University of Chinese Academy of Sciences, No. 19A Yuquan Road, Beijing 100049, China*
[8]*Department of Physics, Federal Urdu University of Arts, Science and Technology, Karachi 75300, Pakistan*

(Received 12 April 2023; accepted 19 July 2024; published 3 September 2024)

The axino, the supersymmetric partner of the axion, is a well-motivated warm/hot dark/cold matter candidate and provides a natural solution to the relic density problem for the binolike neutralino if it is the lightest supersymmetric particle (LSP). With the generalized minimal supergravity, we study such kind of the viable parameter space where the binolike neutralino is the next-to-LSP (NLSP) and the axino is the LSP. In addition, we consider a scenario where the bino is a long-lived NLSP with the lifetime varying from $10^{-6}$ to $10^{-4}$ s and then propose a new signal searching scheme involving one displaced photon together with the large missing transverse momentum at the HL-LHC. The binolike lightest neutralino lies under or around 100 GeV and is produced as a decay product of the right-handed sleptons. The relevant axion coupling $f_a$ can be probed up to $\mathcal{O}(10^9)$ GeV at $2\sigma$ level for the right-handed slepton mass under 800 GeV.

DOI: 10.1103/PhysRevD.110.055006

## I. INTRODUCTION

The Peccei-Quinn (PQ) solution [1,2] stands out among a variety of solutions to the strong $CP$ problem due to its simplicity and elegance. The theory proposed the existence of a global $U(1)$ symmetry that is spontaneously broken at the PQ scale $f_a$. A new Goldstone particle, the axion, is therefore predicted. In the low-energy supersymmetry (SUSY) theory relevant to the PQ solution, the axino, as the supersymmetric partners of the axion [3–8], is considered as an alternative lightest supersymmetric particle (LSP) and thus a dark matter (DM) candidate [9,10]. Meanwhile, a long-held paradigm in searching for DM components is that DM is mostly composed of cold DM. In the theory of SUSY, this translates into the weakly interacting massive particles, e.g., the lightest neutralino. If binolike neutralino is the LSP, which was the most favored scenario in SUSY models with gaugino mass unification at the scale of grand unified theory (GUT), one typically obtains an extremely small annihilation cross section and hence exceedingly large values of the DM relic density, which usually lies 2–4 orders of magnitude above the measured value [10,11]. Such scenario inspires physicists to consider nonthermally produced (NTP) axinos, the LSP [12–30], that inherit the binolike neutralino number density via decay of $\tilde{B} \to \tilde{a}\gamma$ [10,11,31,32]. Therefore, the overwhelming binolike DM relic density is suppressed by a factor of $m_{\tilde{a}}/m_{\tilde{\chi}_1^0}$ [31–33].

On the other hand, the current Large Hadron Collider (LHC) sets strong constraints on the mass of SUSY

*Contact author: zhangwenxing@sjtu.edu.cn
†Contact author: waqasmit@hbpu.edu.cn
‡Contact author: ikhan@itp.ac.cn
§Contact author: tli@itp.ac.cn
‖Contact author: shabbar.raza@fuuast.edu.pk

particles. For instance, the gluino and squarks are excluded around 2 TeV [34,35], and the electroweakinos and sleptons are beyond about a few hundred GeV depending on the assumptions [36]. Moreover, SUSY models inspired by new measurements involving $g_\mu - 2$ [37] indicate the slepton mass around a few hundred GeV to TeV scale (for example, see [38] and references therein).

Among the available scenarios where one can avoid the stringent SUSY search constraints and still remain consistent with ongoing searches is the electroweak supersymmetry (EWSUSY) [39–41], where the squarks and/or gluinos are around a few TeV, while the sleptons, sneutrinos, binos, and winos are within 1 TeV. The Higgsinos (or, say, the Higgs bilinear $\mu$ term) can be either heavy or light. In particular, the EWSUSY can be realized in the generalized minimal supergravity (GmSUGRA) [42,43]. Among current slepton searches with bino as the LSP, most experiments constrain the mass of the mixed state of left- and right-handed sleptons. Only a few experiments set constraints on the "pure" right-handed slepton mass due to the weak interaction between binos and the right-handed sleptons. Constraints from LHC indicate that the mass of left- and right-handed slepton mixtures lies between 400 and 800 GeV given different preconditions [44–49]. However, experiments on the pure right-handed slepton only exclude its mass region lower than about 100 GeV at 95% confidence level (CL) [50–54]. This paper focuses on the pure right-handed slepton search with negligible mixing angle between left- and right-handed sleptons. This article is the continuation of our studies of the supersymmetric standard models under the light of current and future SUSY searches [38,55]. In particular, in Ref. [55] we proposed a search for the relatively heavier right-handed selectron at future lepton colliders with the center-of-mass energy $\sqrt{s} = 240$ GeV and integrated luminosity 3000 fb$^{-1}$ via monophoton channel: $\tilde{e}_R^+ \tilde{e}_R^- \to \tilde{\chi}_1^0(\text{bino}) + \tilde{\chi}_1^0(\text{bino}) + \gamma$. It was shown that, for the Z-pole case where the neutralino mass lies around half Z-boson mass, the right-handed selectron is excluded up to 180 and 210 GeV, respectively, at $3\sigma$ and $2\sigma$, while in the case of Higgs-pole solutions, where the neutralino mass lies around half Higgs mass, the right-handed selectron is excluded up to 140 and 180 GeV, respectively, at $3\sigma$ and $2\sigma$. In this study we consider those solutions that have cold dark matter relic density larger than the Planck2018 $5\sigma$ bounds [56]. Furthermore, we assume that the lightest neutralino (relatively long-lived) serves as the next-to-LSP (NLSP) that decays to the LSP axino and a photon.

SUSY particle searching schemes involving long-lived NLSP decay are usually implemented through reconstructing a displaced vertex via hard jets [57–60], and a few detection signals involving nonpointing photons, light sleptons, and large missing $E_T$ without hard jets induced by decay of light sleptons have not been widely investigated [61–63]. Hence there still exists possibilities that the binolike neutralino lies under 100 GeV and the slepton mass is around a few hundred GeV [55].

In contrast with other SUSY particles, the mass of the axino is model dependent and remains unconstrained both experimentally and theoretically. For example, in a straightforward SUSY version of the Dine-Fischler-Srednicki-Zhitnitsky (DFSZ) model, the axino mass is typically rather small and around ∼MeV. Depending on the model and SUSY breaking scale, the axino mass varies from eV to GeV [64–67]. The NTP axino is produced as a decay product of the NLSP, and it would typically become a relativistic particle when produced unless their masses are degenerated. The axino can then become a warm/hot/cold DM candidate due to the redshift of the Universe depending on the axino mass, reheating temperature, and the type of model [68]. In this paper, we study the case of a cold NTP axino dark matter candidate, which makes up most of the DM relic density in the Universe. We consider the axino mass around $\mathcal{O}(1)$ GeV with a given proper value of $f_a \sim 10^{9}$[1] that makes the NTP axino a possible dominant DM candidate [68,70–72]. In addition, since the axino coupling to the normal matter is strongly suppressed by a coupling of $1/f_a$ [73], all heavier SUSY particles cascade decay to the NLSP instead of the axino LSP. Hence it is reasonable to consider the case that the bino decays to axino and a photon ($\tilde{\chi}_0^1 \to \tilde{a}\gamma$) at colliders with the bino being the NLSP whose mass lies under 100 GeV. In this paper, we focus on the case of a cold axino dark matter candidate, where the NTP axino makes up most of the cold DM in the Universe. Depending on the magnitude of the PQ symmetry breaking scale $f_a$, such scenario offers a new avenue for exploring SUSY and DM physics:

(i) For $f_a \gtrsim 10^{12}$ GeV, the axinos are produced one second later than the big bang. The injection of high-energy hadronic and electromagnetic particles [19,74] can affect the abundance of light elements produced during big bang nucleosynthesis (BBN) [75,76], such that the BBN constraint can be severe, as discussed in Refs. [16,33,72,77].

(ii) For $10^{9-10} \lesssim f_a \lesssim 10^{12}$ GeV, there exists possibilities that the bino NLSP becomes a long-lived particle [59,78,79]. The photon would trigger a delayed timing signal and leave energy depositions in the electromagnetic calorimeter. The signal has a very clean background [61] and therefore deserves to simulate before the running of the HL-LHC. We focus on this scenario in this work.

(iii) For $f_a \lesssim 10^{7-8}$ GeV, the binolike neutralino prompts decays to axino and gamma rays, leaving a signal of two photons plus large missing energy,

[1]The axion properties are related to the PQ symmetry breaking scale with $m_a \simeq 5.7\ \mu\text{eV}(\frac{10^{12}\ \text{GeV}}{f_a})$ [69] and its relic density $\Omega_a = 0.12(\frac{28\ \mu\text{eV}}{m_a})^{7/6}$. In the case of $f_a \sim 10^9$ [69], the axion relic density composes no more than 1% of the DM.

for which the background is very clean at the lepton colliders and is widely investigated in Refs. [16,80–82]. By the way, to evade the cooling constraints from the stars and supernovae, we can assume that the axion has flavor-violating couplings to the Standard Model (SM) fermions, for example, the axion mainly couples to the third generation of the SM fermions. Because the temperatures in the stars and supernovae are not high enough to produce the third generation of the SM fermions, the axions cannot be produced effectively and then the cooling constraints from the stars and supernovae are evaded. Of course, binos can still decay into axinos and photons in this scenario as well.

It is well known that there are two kinds of the viable invisible axion models that can satisfy the experimental bounds: (1) the Kim-Shifman-Vainshtein-Zakharov (KSVZ) axion model, which introduces a SM singlet and a pair of extra vectorlike quarks that are charged under $U(1)_{PQ}$, while the SM fermions and Higgs fields are neutral [5,6]; (2) the DFSZ axion model, in which a SM singlet and one pair of Higgs doublets are introduced, and the SM fermions and Higgs fields are all charged under $U(1)_{PQ}$ symmetry [7,8]. In this paper, we shall consider the DFSZ axion model and a SUSY scenario, where the bino is a long-lived NLSP with the lifetime varying from $10^{-6}$ to $10^{-4}$ s, and then propose a new signal searching scheme involving one displaced photon together with the large missing transverse momentum at the High Luminosity LHC (HL-LHC). The binolike lightest neutralino lies under or around 100 GeV and is produced as a decay product of the right-handed sleptons. The relevant axion coupling $f_a$ can be probed up to $\mathcal{O}(10^9)$ GeV at $2\sigma$ level for the right-handed slepton mass under 300 GeV and the lightest neutralino mass under 100 GeV. Also, the KSVZ model can be discussed similarly.

This paper is organized as follows. Section II introduce the framework of the GmSUGRA model. Section IV presents the variable scanning parameter space. In Sec. V, we discuss the related collider analysis and the kinetic variables. At the end of this section, numerical results are presented. Conclusions are presented in the last section.

## II. THE GMSUGRA MODEL

In this study we consider the simple GmSUGRA where the GUT gauge group is $SU(5)$ and the Higgs field $\Phi$ for the GUT symmetry breaking is in the $SU(5)$ adjoint representation [42,43]. The scalar masses and trilinear soft terms will be modified as well due to the relevant high-dimensional operators [43]. It should be noted that, since $\Phi$ can couple to the gauge field kinetic terms via high-dimensional operators, the gauge coupling relation and gaugino mass relation at the GUT scale will be modified after $\Phi$ acquires a vacuum expectation value [42,83]. The gauge coupling relation and gaugino mass relation at the GUT scale are given as [42,83]

$$\frac{1}{\alpha_2}-\frac{1}{\alpha_3}=k\left(\frac{1}{\alpha_1}-\frac{1}{\alpha_3}\right), \tag{1}$$

$$\frac{M_2}{\alpha_2}-\frac{M_3}{\alpha_3}=k\left(\frac{M_1}{\alpha_1}-\frac{M_3}{\alpha_3}\right), \tag{2}$$

where $k$ is the index of these relations and is equal to $5/3$ [42] in our simple GmSUGRA. Such gauge coupling relation and gaugino mass relation at the GUT scale can be realized in the F-theory $SU(5)$ models, where the gauge symmetry is broken down to the SM gauge symmetry by turning on the $U(1)_Y$ flux, and the F-theory $SO(10)$ models, where the gauge symmetry is broken down to the $SU(3)_C \times SU(2)_L \times SU(2)_R \times U(1)_{B-L}$ gauge symmetry by turning on the $U(1)_{B-L}$ flux [84]. The point is that the $U(1)_Y$ and $U(1)_{B-L}$ fluxes can give extra contributions to the gauge kinetic terms of the SM gauge fields.

We assume for simplicity that at the GUT scale $\alpha_1 = \alpha_2 = \alpha_3$ and then the gaugino mass relation becomes

$$M_2 - M_3 = \frac{5}{3}(M_1 - M_3). \tag{3}$$

The expression for $M_3$ may be written in terms of $M_1$ and $M_2$ as follows:

$$M_3 = \frac{5}{2}M_1 - \frac{3}{2}M_2. \tag{4}$$

So there are two free parameters in gaugino masses. To realize the electroweak supersymmetry, we require that $M_3$ be larger than $M_1$ and $M_2$.

In addition, the supersymmetry breaking scalar masses at the GUT scale are [39,43]

$$m^2_{\tilde{Q}_i} = (m_0^U)^2 + \sqrt{\frac{3}{5}}\beta'_{\mathbf{10}}\frac{1}{6}(m_0^N)^2, \tag{5}$$

$$m^2_{\tilde{U}^c_i} = (m_0^U)^2 - \sqrt{\frac{3}{5}}\beta'_{\mathbf{10}}\frac{2}{3}(m_0^N)^2, \tag{6}$$

$$m^2_{\tilde{E}^c_i} = (m_0^U)^2 + \sqrt{\frac{3}{5}}\beta'_{\mathbf{10}}(m_0^N)^2, \tag{7}$$

$$m^2_{\tilde{D}^c_i} = (m_0^U)^2 + \sqrt{\frac{3}{5}}\beta'_{\bar{\mathbf{5}}}\frac{1}{3}(m_0^N)^2, \tag{8}$$

$$m^2_{\tilde{L}_i} = (m_0^U)^2 - \sqrt{\frac{3}{5}}\beta'_{\bar{\mathbf{5}}}\frac{1}{2}(m_0^N)^2, \tag{9}$$

$$m^2_{\tilde{H}_u} = (m_0^U)^2 + \sqrt{\frac{3}{5}}\beta'_{Hu}\frac{1}{2}(m_0^N)^2, \tag{10}$$

$$m^2_{\tilde{H}_d} = (m_0^U)^2 - \sqrt{\frac{3}{5}}\beta'_{Hd}\frac{1}{2}(m_0^N)^2, \tag{11}$$

where $i$ is the generation index, $\beta'_{\mathbf{10}}$, $\beta'_{\bar{\mathbf{5}}}$, $\beta'_{Hu}$, and $\beta'_{Hd}$ are coupling constants, and $m_0^U$ and $m_0^N$ are the scalar masses related to the universal and nonuniversal parts, respectively. In particular, the squark masses can be much larger than the slepton masses since the cancellations between the two terms in the slepton masses $m^2_{\tilde{E}_i^c}$ and $m^2_{\tilde{L}_i^c}$ can be realized by a little bit of fine-tuning of $\beta'_{\mathbf{10}}$ and $\beta'_{\bar{\mathbf{5}}}$, respectively. Also, the supersymmetry breaking soft masses $m^2_{\tilde{H}_u}$ and $m^2_{\tilde{H}_d}$ can be free parameters as well.

Interestingly, we can derive the scalar mass relations at the GUT scale

$$\begin{aligned} 3m^2_{\tilde{D}_i^c} + 2m^2_{\tilde{L}_i} &= 4m^2_{\tilde{Q}_i} + m^2_{\tilde{U}_i^c} = 6m^2_{\tilde{Q}_i} - m^2_{\tilde{E}_i^c} \\ &= 2m^2_{\tilde{E}_i^c} + 3m^2_{\tilde{U}_i^c}. \end{aligned} \tag{12}$$

Choosing slepton masses as input parameters, we can parametrize the squark masses as follows:

$$m^2_{\tilde{Q}_i} = \frac{5}{6}(m_0^U)^2 + \frac{1}{6}m^2_{\tilde{E}_i^c}, \tag{13}$$

$$m^2_{\tilde{U}_i^c} = \frac{5}{3}(m_0^U)^2 - \frac{2}{3}m^2_{\tilde{E}_i}, \tag{14}$$

$$m^2_{\tilde{D}_i^c} = \frac{5}{3}(m_0^U)^2 - \frac{2}{3}m^2_{\tilde{L}_i}. \tag{15}$$

In short, the squark masses can be parametrized by the slepton masses and the universal scalar mass. If the slepton masses are much smaller than the universal scalar mass, we obtain $2m^2_{\tilde{Q}_i} \sim m^2_{\tilde{U}_i^c} \sim m^2_{\tilde{D}_i^c}$.

Moreover, we can calculate the supersymmetry breaking trilinear soft $A$ terms $A_U$, $A_D$, and $A_E$, respectively, for the SM fermion Yukawa superpotential terms of the up-type quarks, down-type quarks, and charged leptons at the GUT scale [43]

$$A_U = A_0^U + (2\gamma_U + \gamma'_U)A_0^N, \tag{16}$$

$$A_D = A_0^U + \frac{1}{6}\gamma_D A_0^N, \tag{17}$$

$$A_E = A_0^U + \gamma_D A_0^N, \tag{18}$$

where $\gamma_U$, $\gamma'_U$, and $\gamma_D$ are coupling constants, and $A_0^U$ and $A_0^N$ are the corresponding trilinear soft $A$ terms related to the universal and nonuniversal parts, respectively. Therefore, $A_U$, $A_D$, and $A_E$ can be free parameters, in general, in the GmSUGRA.

In short, we can parametrize the generic supersymmetry breaking soft mass terms at the GUT scale in our simple GmSUGRA as following: two parameters in the gaugino masses, three parameters for the squark and slepton soft masses, three parameters in the trilinear soft $A$ terms, and two parameters for the Higgs soft masses. The $\mu$ and its soft term $B_\mu$ are determined by the $M_Z$ and $\tan\beta$ from electroweak symmetry breaking. Thus, including $\tan\beta$ we have 11 parameters in the most general case. Since we assume $A_U = A_D$, we have ten input parameters.

As shown in Ref. [39] and can also be seen in this study for the electroweak supersymmetry in GmSUGRA: the squarks and/or gluinos are heavy around a few TeV, while the sleptons, binos, and winos are light and within 1 TeV. The Higgsinos (or $\mu$ term) can be either heavy or light. Thus, both the gaugino masses $M_1$ and $M_2$ and the slepton/sneutrino soft masses are smaller than or around 1 TeV.

## III. SCANNING PROCESS

In order to carry out random scans over the parameter space described below, we make use of the ISAJET 7.84 software package. Through the use of the Minimal Supersymmetric Standard Model (MSSM) renormalization group equations in the $\overline{DR}$ regularization scheme, the weak scale values of the gauge and third generation Yukawa couplings are evolved in this package to the value $M_{\rm GUT}$. We do not strictly enforce the unification condition $g_3 = g_1 = g_2$ at $M_{\rm GUT}$ since a few percent departure from unification may be allocated to the unknown GUT scale threshold corrections. All of the soft susy breaking parameters (SSB) parameters, together with the gauge and Yukawa couplings, are evolved back to the weak scale $M_Z$ when the boundary conditions are specified as $M_{\rm GUT}$. See [85] for more details on the workings of ISAJET.

Using parameters given in Sec. II, we perform the random scans for the following parameter ranges:

$$\begin{aligned} 100 \le m_0^U &\le 5000 \text{ GeV}, \\ 80 \le M_1 &\le 400 \text{ GeV}, \\ 600 \le M_2 &\le 1200 \text{ GeV}, \\ 600 \le m_{\tilde{L}} &\le 1200 \text{ GeV}, \\ 100 \le m_{\tilde{E}^c} &\le 350 \text{ GeV}, \\ 100 \le m_{\tilde{H}_{u,d}} &\le 5000 \text{ GeV}, \\ -6000 \le A_U = A_D &\le 6000 \text{ GeV}, \\ -600 \le A_E &\le 600 \text{ GeV}, \\ 2 \le \tan\beta &\le 60. \end{aligned} \tag{19}$$

We have also considered $\mu \ge 0$ and used $m_t = 173.3$ GeV. All the data gathered are Radiative Electroweak Symmetry Breaking (REWSB) compatible, with the neutralino serving as the LSP. To properly interpret the results, we need the following constraints (motivated by the LEP2 experiment) on sparticle masses.

LEP constraints: We impose the bounds that the LEP2 experiments set on charged sparticle masses ($\gtrsim$100 GeV) [86].

Higgs boson mass: The experimental combination for the Higgs mass reported by the ATLAS and CMS Collaborations is [87]

$$m_h = 125.09 \pm 0.21(\text{stat}) \pm 0.11(\text{syst}) \text{ GeV}. \quad (20)$$

Because of the theoretical uncertainty in the Higgs mass calculations in the MSSM—see, e.g., [88,89]—we apply the constraint from the Higgs boson mass to our results as

$$122 \leq m_h \leq 128 \text{ GeV}. \quad (21)$$

Rare $B$-meson decays: Since the SM predictions are in good agreement with the experimental results for the rare decays of $B$ mesons such as the $B_s \to \mu^+\mu^-$, $B_s \to X_s\gamma$, where $X_s$ is an appropriate state including a strange quark, the results of our analyses are required to be consistent with the measurements for such processes. Thus, we employ the following constraints from B physics [90,91]:

$$1.6 \times 10^{-9} \leq \text{BR}(B_s \to \mu^+\mu^-) \leq 4.2 \times 10^{-9}, \quad (22)$$

$$2.99 \times 10^{-4} \leq \text{BR}(b \to s\gamma) \leq 3.87 \times 10^{-4}, \quad (23)$$

$$0.70 \times 10^{-4} \leq \text{BR}(B_u \to \tau\nu_\tau) \leq 1.5 \times 10^{-4}. \quad (24)$$

Current LHC searches: Based on [92–97], we consider the following constraints on gluino and first/second generation squark masses

$$m_{\tilde{g}} \gtrsim 2.2, \qquad m_{\tilde{q}} \gtrsim 2, \qquad m_{\tilde{t}_1} \gtrsim 1.2 \text{ TeV}. \quad (25)$$

DM searches and relic density: We apply the following limit for the neutralino relic density in order to facilitate the discussion on the phenomenology of the axino DM in our scenario:

$$\Omega_{\tilde{\chi}_1^0} h^2 \gtrsim 0.126. \quad (26)$$

## IV. SCANS RESULTS

In this section we show results of our scans only for the relevant parameters. In Fig. 1, the plot in the left panel shows neutralino relic density ($\Omega_{\tilde{\chi}_1^0} h^2$) as a function of NLSP neutralino mass. Here we have made sure that $\Omega_{\tilde{\chi}_1^0} h^2 \gtrsim 0.126$ (greater than the Planck2018 $5\sigma$ bounds). It is evident from the plot that in our scans $\Omega_{\tilde{\chi}_1^0} h^2$ can be as large as 1000, while $m_{\tilde{\chi}_1^0}$ is between 20 and 170 GeV. In the right panel, we show the plot in the $m_{\tilde{\chi}_1^0}$–$m_{\tilde{a}}$ plane. As we stated above, in this study we consider nonthermally produced axinos that dominate the dark matter relic density. In that case, we assume the case in which the NLSP neutralino decays to the LSP axino and a photon such that $\Omega_{\tilde{a}}^{\text{NTP}} h^2 \approx 0.11$. Thus, in such a scenario we calculate axino mass as $m_{\tilde{a}} \approx \frac{\Omega_{\tilde{a}}^{\text{NTP}} h^2}{\Omega_{\tilde{\chi}_1^0} h^2} m_{\tilde{\chi}_1^0}$ [77]. We see that, in our scans, axino mass can be very light, but can be as heavy as 90 GeV. We then use the $m_{\tilde{\chi}_1^0}$ and $m_{\tilde{a}}$ to calculate the width $\Gamma(\tilde{\chi}_1^0 \to \tilde{a}\gamma)$ as shown in the next section.

## V. LONG-LIVED AXINO SEARCHES AT THE LHC

As the LSP, the axino can be produced by the decay of the unstable NLSP, the lightest neutralino. The width $\Gamma(\tilde{\chi}_1^0 \to \tilde{a}\gamma)$ has been calculated in Refs. [72,77] and is given by

$$\Gamma(\tilde{\chi}_1^0 \to \tilde{a}\gamma) = \frac{\alpha_{em}^2 C_{aYY}^2 v_4^{(1)2}}{128\pi^3 \cos^2\theta_W} \frac{m_{\tilde{\chi}_1^0}^3}{(f_a/N)^2} \left(1 - \frac{m_{\tilde{a}}^2}{m_{\tilde{\chi}_1^0}^2}\right), \quad (27)$$

where $v_4^{(1)}$ denotes the bino fraction of neutralino of $\tilde{\chi}_1^0$, $N$ is the model-dependent anomaly factor of order $\mathcal{O}(1)$, and $C_{aYY}$ (e.g., $C_{aYY} = 8/3$ in the DFSZ model) is a model-dependent coupling factor. In the following text, without loss of generality, we consider the DFSZ model as an

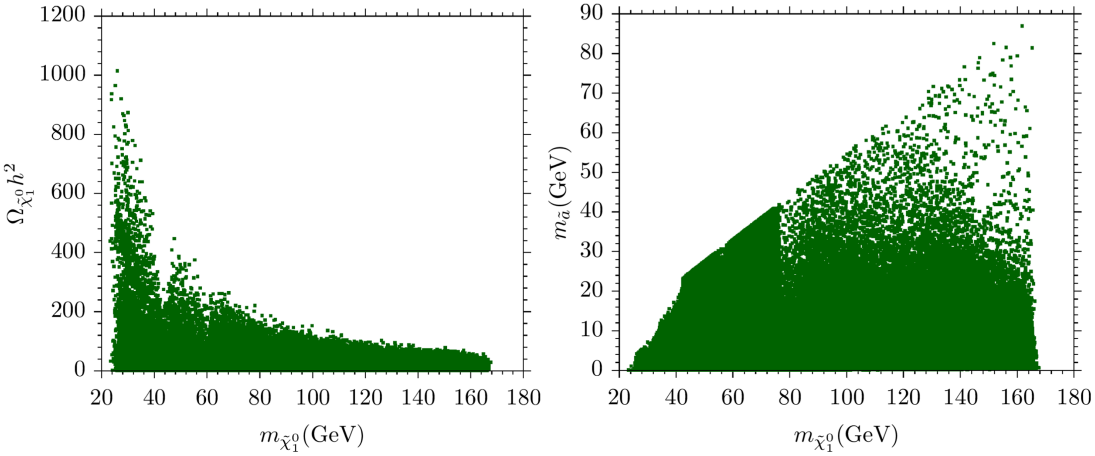


FIG. 1. Plots in $m_{\tilde{\chi}_1^0} - \Omega_{\tilde{\chi}_1^0} h^2$ (left) and $m_{\tilde{\chi}_1^0}$–$m_{\tilde{a}}$ planes. All the points satisfy REWSB bounds, particle mass bounds, B-physics bounds, and $\Omega_{\tilde{\chi}_1^0} \gtrsim 0.126$ as described in Sec. IV.

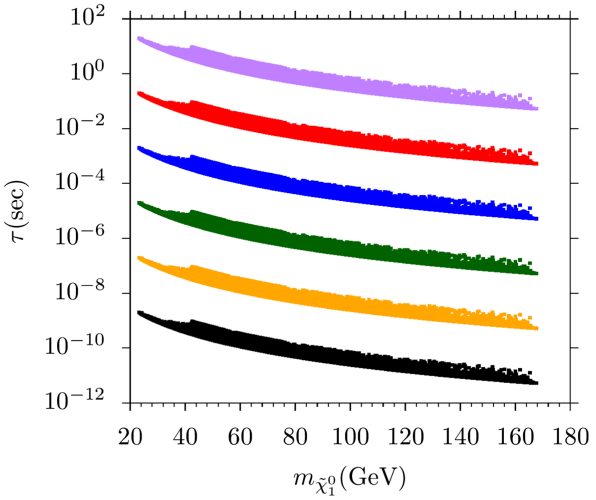


FIG. 2. Lifetimes in seconds of the lightest neutralino versus its mass for $f_a/N = 10^7, 10^8, 10^9, 10^{10}, 10^{11}$, and $10^{12}$ GeV from the bottom to the top.

example. One can check the average decay length of the lightest neutralino lies within 1 m when $f_a/N \lesssim 10^7$ GeV. However, even if the $f_a/N \sim 10^8$ and $10^9$ GeV, there still exists the possibility that the lightest neutralinos decay within the electromagnetic calorimeter (ECAL) and thus is able to be detected. On the other hand, in the case of $f_a/N \gtrsim 10^8$ and $10^9$ GeV, events would be more likely to escape from the current constraints of LHC. Hence, the parameter space with $f_a/N \sim 10^8$ and $10^9$ GeV is essential in searching for the long-lived neutralino signal. In fact, our simulation has shown the parameter region with $f_a/N \lesssim 10^7$ GeV has been excluded by the LHC searches. In Fig. 2, we plot the $\tilde{\chi}_1^0$ lifetime in seconds versus $m_{\tilde{\chi}_1^0}$ for six choices of $f_a/N$ and taking $C_{aYY} = 8/3$ in the DFSZ model.

The NLSP decay length depends on the PQ symmetry breaking scale $f_a$ and then provides important information about the $U(1)$ symmetry breaking mechanism. The very weak coupling of the NLSP to the axino could lead to the displaced vertices (DVs) of the NLSP. In this case, photons are generated in the point of DVs, and they reach the ECAL up to $\mathcal{O}(1)$ ns later than particles generated in the primary vertex. Thus, measuring the photon time of arrival delay with respect to a photon produced at the primary vertex and traveling at the speed of light helps to discriminate between signal and background. Since the best time resolution for the ECAL is measured to be between 70 and 100 ps [98], the ECAL is able to detect the delayed arrived photons.

In our model, at the LHC, the axino can be generated by the cascade decay of the right-handed (RH) sleptons, and the concomitant decay product, the photon, is able to be distinguished by the ECAL due to the delayed arrival time.

At the HL-LHC, a characteristic signal process associated with the generation of the long-lived neutralino is $pp \to \tilde{l}_R^- \tilde{l}_R^+ \to l_R^+ l_R^- \tilde{\chi}_1^0 \tilde{\chi}_1^0$ with the slepton being an on-shell

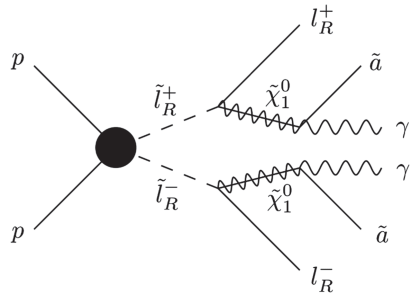


FIG. 3. A characteristic signal process associated with the generation of the long-lived neutralino.

particle, see Fig. 3. In the simulation, we generate the signal process and calculate the possibility for the NLSP $\tilde{\chi}_1^0$ to decay inside the ECAL.

The geometrical acceptance probability for the LSP with a decay length $d$ as it traverses the detector is given by

$$p = \frac{1}{4\pi} \int_{\Delta\Omega} d\Omega \int_{L_1}^{L_2} \frac{1}{d} e^{-L/d}, \tag{28}$$

where $L_1$ and $L_2$ are the distances between the interaction point to the point where the long-lived particle (LLP) enters and exits the decay volume, and $\Delta\Omega$ is the solid angle of the active detector volume [99,100]. In our simulation, $L_1$ is chosen to be the interaction point, $L_2$ is the point for $\tilde{\chi}_1^0$ to exit the ECAL, and $\Delta\Omega$ is the solid angle covered by the ECAL barrel.

As for the photons, they can be detected by the barrel region of the ECAL detector ($|\eta| < 1.444$) with its mother particle $p_T > 70$ GeV labeled as tight photons [98]. On the other hand, the photons, which can be detected by the whole region of the ECAL detector ($|\eta| < 2.37$) with its mother particle $p_T > 50$ GeV, are labeled as loose photons [62]. Both photons are required to be isolated, by requiring

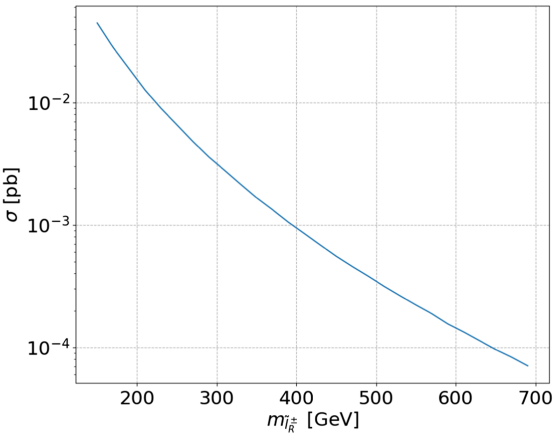


FIG. 4. The RH slepton associated with $\tilde{a}$ production cross section at the HL-LHC with the collision energy $\sqrt{s} = 14$ TeV and the integrated luminosity of 3000 fb$^{-1}$.

that the transverse energy be deposited in the calorimeter in a cone of radius $\Delta R = \sqrt{(\Delta\eta)^2 + (\Delta\phi)^2} = 0.4$.

The Monte Carlo samples of signal events are generated by using the MadGraph5 [101] for hard scattering processes, PYTHIA 8.2 [102] for parton showering and hadronization, and DELPHES 3 [103] for jet clustering and detector simulation. We generate signal events with collider collision energy being 14 TeV and the luminosity set to be 3000 fb$^{-1}$. In Fig. 4, we plot the axino production cross section in picobarn versus $m_{\tilde{l}_R}$ at the HL-LHC with the lightest neutralino set to be $m_{\tilde{\chi}_1^0} = 50$ GeV. Since the slepton decays to $\tilde{\chi}_1^0$ by 100%, the axino production cross section is independent of $m_{\tilde{\chi}_1^0}$ at tree level. In addition, the signal processes with $m_{\tilde{\chi}_1^0} > 500$ GeV generate event number less than $\mathcal{O}(1)$ by 3000 fb$^{-1}$ luminosity and thus induce a considerable statistical error. Hence, in simulation, we consider the LSP mass ranging from 50 to 130 GeV in steps of 10 GeV, and the right-handed slepton mass from 150 to 500 GeV in steps of 20 GeV. The signal events with two tight photons are selected out. With the above calculation of LLP decay possibility, we can then estimate 95% CL exclusion limits under the assumption of zero background in the RH slepton and neutralino mass planes.

As indicated in Eq. (27), the decay length of $\tilde{\chi}_1^0$ becomes larger as the PQ scale $f_a$ grows. For larger $f_a/N$, the neutralino $\tilde{\chi}_1^0$ is more likely to decay outside the ECAL. In Fig. 5, the PQ breaking scale is chosen to be between $f_a/N = 8.0 \times 10^8$ and $4.0 \times 10^9$ GeV. The solid black line is the expected exclusion limit on the right-handed slepton searches at the HL-LHC, which is obtained by extrapolation from the left- and right-handed slepton limit at the LHC [49] to the right-handed slepton limit with 14 TeV, 3000 fb$^{-1}$. Points under the line are excluded. Each point requires a complete simulation, discussed in Sec. V. Searching for the long-lived neutralino improves the right-handed slepton detection efficiency significantly. For $f_a/N \sim 10^9$ GeV, the $l_R^{\pm}$ is excluded around 800 GeV and the $\tilde{\chi}_1^0$ excluded up to about 600 GeV at 95% CL. As we pointed out above, we consider the DFSZ model as an example. For the KSVZ model with $C'_{aYY} \neq \frac{8}{3}$, the lower limit on $f_a/N$ will be rescaled by a factor of $v_4^{(1)} C'_{aYY}/C_{aYY}$.

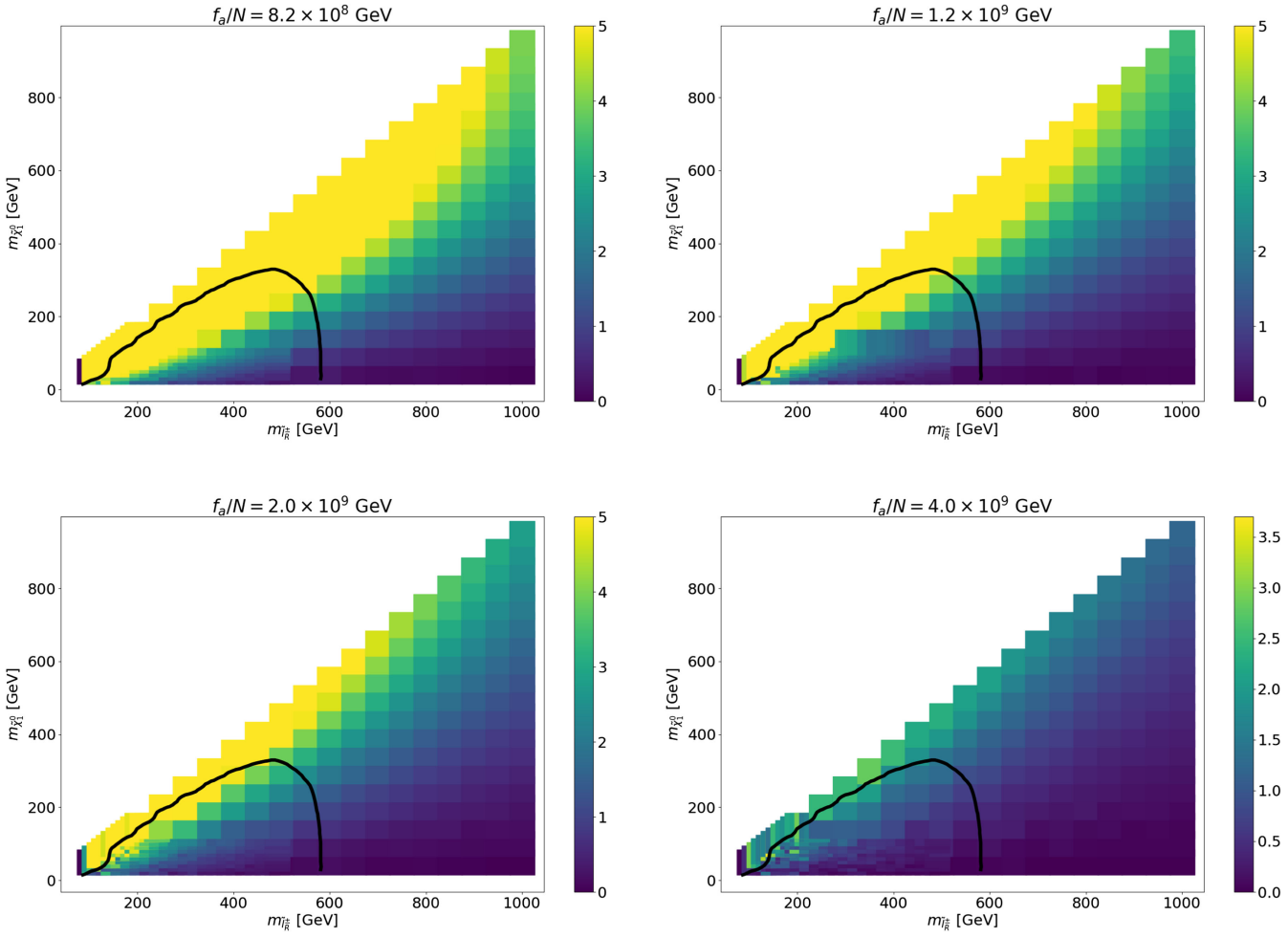


FIG. 5. The signal significance for the axino $\tilde{a}$ to be detected by the ECAL.

TABLE I. The PQ symmetry breaking scales ($f_a$), decay width ($\Gamma$), sparticle and Higgs masses in GeV, as well as lifetimes (LT) in seconds.

| | Point 1 | Point 2 | Point 3 | Point 4 | Point 5 |
|---|---|---|---|---|---|
| $m_0^U$ | 1927 | 1285 | 2496 | 2111 | 1502 |
| $M_1$ | 116.1 | 238.5 | 153.9 | 186.9 | 220.3 |
| $M_2$ | −814.6 | −635.5 | −1148 | −1014 | −872.9 |
| $M_3$ | 1512.1 | 1549.5 | 2106.8 | 1988.2 | 1860.1 |
| $m_{E^c}, m_L$ | 292.6, 1121 | 154.1, 883.8 | 114.8, 670.5 | 207.5, 1041 | 294.9, 713.2 |
| $m_Q$ | 1763.2 | 1174.7 | 2279 | 1928.9 | 1376.4 |
| $m_{U^c}$ | 2476.2 | 1654.1 | 3221 | 2720 | 1924.1 |
| $m_{D^c}$ | 2487.7 | 1658.9 | 3222.3 | 2725.3 | 1939.1 |
| $m_{H_u}, m_{H_d}$ | 1025, 1286 | 183.7, 1442 | 2653, 1551 | 2325, 1566 | 3807, 3069 |
| $A_t = A_b, A_\tau$ | −5974, 61.96 | −5944, −365.3 | −2459, −126.8 | −5380, 260.7 | −2787, 559.5 |
| $\tan\beta$ | 6.77 | 44.1 | 41.7 | 11.8 | 22 |
| $m_h$ | 123 | 125 | 122 | 122 | 125 |
| $m_H$ | 3437 | 2133 | 3414 | 3839 | 4096 |
| $m_A$ | 3415 | 2120 | 3392 | 3814 | 4069 |
| $m_{H^\pm}$ | 3438 | 2135 | 3415 | 3840 | 4097 |
| $m_{\tilde{\chi}^0_{1,2}}$ | 44, 725 | 98, 569 | 55, 1015 | 71, 905 | 87, 775 |
| $m_{\tilde{\chi}^0_{3,4}}$ | 3234, −3234 | 2895, 2896 | −3009, 3010 | 3101, 3101 | 2108, 2108 |
| $m_{\tilde{\chi}^\pm_{1,2}}$ | 729, 3247 | 571, 2900 | 1017, 3009 | 910, 3106 | 779, 2113 |
| $m_{\tilde{g}}$ | 3320 | 3344 | 4517 | 4262 | 3966 |
| $m_{\tilde{u}_{L,R}}$ | 3349, 3685 | 3125, 3297 | 4481, 4903 | 4129, 4448 | 3852, 3701 |
| $m_{\tilde{t}_{1,2}}$ | 2230, 2705 | 1781, 2226 | 3786, 4028 | 3324, 3617 | 2212, 2877 |
| $m_{\tilde{d}_{L,R}}$ | 3450, 3773 | 3127, 3335 | 4481, 5013 | 4130, 4550 | 3701, 3940 |
| $m_{\tilde{b}_{1,2}}$ | 2672, 3730 | 2174, 2837 | 3828, 4700 | 3579, 4487 | 2870, 3708 |
| $m_{\tilde{\nu}_1}$ | 1098 | 907 | 645 | 1021 | 700 |
| $m_{\tilde{\nu}_3}$ | 1096 | 924 | 391 | 1006 | 549 |
| $m_{\tilde{e}_{L,R}}$ | 1106, 816 | 914, 492 | 635, 1032 | 1029 | 724, 810 |
| $m_{\tilde{\tau}_{1,2}}$ | 814, 1102 | 454, 947 | 240, 740 | 900, 1020 | 485, 616 |
| $f_a$ | $10^8$ | $10^8$ | $10^9$ | $10^{10}$ | $10^{11}$ |
| $m_{\tilde{a}}$ | 0.055 | 1.995 | 1.993 | 0.09 | 0.652 |
| $\Omega_{\tilde{\chi}} h^2$ | 86.855 | 5.38 | 3.044 | 87.25 | 14.69 |
| $\Gamma(\tilde{\chi}^0_1 \to \tilde{a}\gamma)$ | $2.22 \times 10^{-17}$ | $2.49 \times 10^{-16}$ | $4.46 \times 10^{-19}$ | $9.65 \times 10^{-21}$ | $1.8 \times 10^{-22}$ |
| LT | $2.97 \times 10^{-8}$ | $2.65 \times 10^{-9}$ | $1.47 \times 10^{-6}$ | $6.82 \times 10^{-5}$ | $3.74 \times 10^{-3}$ |

Before concluding our paper we also display five benchmark points in Table I as examples of bino NLSP. Points 1 and 2 represent a scenario for $f_a = 10^8$ GeV. Here we see that the bino NLSP lifetime is on the order of $10^{-8}$ and $10^{-9}$ s, respectively. This means that the bino NLSP will decay just beyond or within the ECAL. In rest of the benchmark points, the bino NLSP will decay well beyond the ECAL.

## VI. CONCLUSION

The supersymmetric PQ models, which solve the strong *CP* problem and provide viable DM candidates simultaneously, are also compelling from the collider phenomenological point of view. On the one hand, the inclusion of the axino LSP provides a natural solution to the density problem for the binolike lightest neutralino. On the other hand, the axino is hard to be produced directly by the SM particle collision due to the coupling suppression $1/f_a$, and the axino is, therefore, usually produced via the SUSY particle decays at colliders. If the axion coupling lies between $10^{9\text{–}10}$ GeV $\lesssim f_a \lesssim 10^{12}$, the lightest neutralino may become a long-lived particle and hence provide a unique signal with very clean background at hadron colliders. However, the analysis scheme to search for production of the axino LSP via light slepton decay at hadron colliders is inadequately investigated, whose final states include hard leptons, displaced photons, and large missing energy. The lack of hard jets makes the displaced vertex difficult to be reconstructed. In this paper, we concentrated on the scenario where the slepton is a few hundred GeV and the binolike lightest neutralino mass is under or around 100 GeV, as well as proposed a new analysis method to search for the signal of the long-lived neutralino. In the analyses, we considered the DFSZ model as an example and calculated the possibility that the binolike

NLSP decays inside the ECAL, assuming zero background. We found that, for $f_a/N \sim 10^9$ GeV, the right-handed slepton $l_R^{\pm}$ can be excluded around 200 GeV, and the binolike lightest neutralino $\tilde{\chi}_0^1$ can excluded up to about 80 GeV within $2\sigma$ deviation.

## ACKNOWLEDGMENTS

This research is supported in part by the National Key Research and Development Program of China Grant No. 2020YFC2201504, by the Projects No. 11875062, No. 11947302, No. 12047503, and No. 12275333 supported by the National Natural Science Foundation of China, by the Key Research Program of the Chinese Academy of Sciences, Grant No. XDPB15, by the Scientific Instrument Developing Project of the Chinese Academy of Sciences, Grant No. YJKYYQ20190049, and by the International Partnership Program of Chinese Academy of Sciences for Grand Challenges, Grant No. 112311KYSB20210012.

[1] R. D. Peccei and H. R. Quinn, *CP* conservation in the presence of instantons, Phys. Rev. Lett. **38**, 1440 (1977).
[2] R. D. Peccei and H. R. Quinn, Constraints imposed by *CP* conservation in the presence of instantons, Phys. Rev. D **16**, 1791 (1977).
[3] S. Weinberg, A new light boson?, Phys. Rev. Lett. **40**, 223 (1978).
[4] F. Wilczek, Problem of strong *P* and *T* invariance in the presence of instantons, Phys. Rev. Lett. **40**, 279 (1978).
[5] J. E. Kim, Weak interaction singlet and strong *CP* invariance, Phys. Rev. Lett. **43**, 103 (1979).
[6] M. A. Shifman, A. I. Vainshtein, and V. I. Zakharov, Can confinement ensure natural *CP* invariance of strong interactions?, Nucl. Phys. **B166**, 493 (1980).
[7] M. Dine, W. Fischler, and M. Srednicki, A simple solution to the strong *CP* problem with a harmless axion, Phys. Lett. **104B**, 199 (1981).
[8] A. R. Zhitnitsky, On possible suppression of the axion hadron interactions (in Russian), Sov. J. Nucl. Phys. **31**, 260 (1980).
[9] J. Preskill, M. B. Wise, and F. Wilczek, Cosmology of the invisible axion, Phys. Lett. **120B**, 127 (1983).
[10] H. Baer, K.-Y. Choi, J. E. Kim, and L. Roszkowski, Dark matter production in the early Universe: Beyond the thermal WIMP paradigm, Phys. Rep. **555**, 1 (2015).
[11] L. Roszkowski, E. M. Sessolo, and S. Trojanowski, WIMP dark matter candidates and searches—current status and future prospects, Rep. Prog. Phys. **81**, 066201 (2018).
[12] A. Monteux and C. S. Shin, Axino LSP baryogenesis and dark matter, J. Cosmol. Astropart. Phys. 05 (2015) 035.
[13] G. Barenboim, E. J. Chun, S. Jung, and W. I. Park, Implications of an axino LSP for naturalness, Phys. Rev. D **90**, 035020 (2014).
[14] E. J. Chun, Axino phenomenology, Eur. Phys. J. Spec. Topics **229**, 3221 (2020).
[15] K.-Y. Choi, J. E. Kim, and L. Roszkowski, Review of axino dark matter, J. Korean Phys. Soc. **63**, 1685 (2013).
[16] A. Freitas, F. D. Steffen, N. Tajuddin, and D. Wyler, Axinos in cosmology and at colliders, J. High Energy Phys. 06 (2011) 036.
[17] C. Cheung, G. Elor, and L. J. Hall, The cosmological axino problem, Phys. Rev. D **85**, 015008 (2012).
[18] A. Strumia, Thermal production of axino dark matter, J. High Energy Phys. 06 (2010) 036.
[19] A. Freitas, F. D. Steffen, N. Tajuddin, and D. Wyler, Upper limits on the Peccei-Quinn scale and on the reheating temperature in axino dark matter scenarios, Phys. Lett. B **679**, 270 (2009).
[20] L. Covi and J. E. Kim, Axinos as dark matter particles, New J. Phys. **11**, 105003 (2009).
[21] F. D. Steffen, Dark matter candidates—axions, neutralinos, gravitinos, and axinos, Eur. Phys. J. C **59**, 557 (2009).
[22] J. U. Kang and G. Panotopoulos, Dark matter in supersymmetric models with axino LSP in Randall-Sundrum II brane model, J. High Energy Phys. 05 (2008) 036.
[23] J. E. Kim, Axion as a CDM component, in *Proceedings of the 23rd International Symposium on Lepton-Photon Interactions at High Energy (LP07), Daegu, South Korea* (2007), pp. 408–420.
[24] K.-Y. Choi, L. Roszkowski, and R. Ruiz de Austri, Determining reheating temperature at colliders with axino or gravitino dark matter, J. High Energy Phys. 04 (2008) 016.
[25] L. Roszkowski and O. Seto, Axino dark matter from *Q*-balls in Affleck-Dine baryogenesis and the $\Omega_b - \Omega_{\rm DM}$ coincidence problem, Phys. Rev. Lett. **98**, 161304 (2007).
[26] S. Kasuya, E. Kawakami, and M. Kawasaki, Axino dark matter and baryon number asymmetry production by the *Q*-ball decay in gauge mediation, J. Cosmol. Astropart. Phys. 03 (2016) 011.
[27] L. Roszkowski, S. Trojanowski, and K. Turzynski, Axino and gravitino dark matter with low reheating temperature, Proc. Sci. EPS-HEP2015 (**2015**) 398.
[28] L. Roszkowski, S. Trojanowski, and K. Turzynski, Axino dark matter with low reheating temperature, J. High Energy Phys. 11 (2015) 139.
[29] S. P. Liew, Axino dark matter in light of an anomalous X-ray line, J. Cosmol. Astropart. Phys. 05 (2014) 044.
[30] K.-Y. Choi and O. Seto, X-ray line signal from decaying axino warm dark matter, Phys. Lett. B **735**, 92 (2014).
[31] H. Baer, M. Haider, S. Kraml, S. Sekmen, and H. Summy, Cosmological consequences of Yukawa-unified SUSY with mixed axion/axino cold and warm dark matter, J. Cosmol. Astropart. Phys. 02 (**2009**) 002.

[32] A. Boyarsky, J. Lesgourgues, O. Ruchayskiy, and M. Viel, Lyman-$\alpha$ constraints on warm and on warm-plus-cold dark matter models, J. Cosmol. Astropart. Phys. 05 (2009) 012.
[33] L. Covi, L. Roszkowski, R. Ruiz de Austri, and M. Small, Axino dark matter and the CMSSM, J. High Energy Phys. 06 (2004) 003.
[34] G. Aad *et al.*, Search for squarks and gluinos in final states with jets and missing transverse momentum using 139 fb$^{-1}$ of $\sqrt{s} = 13$ TeV $pp$ collision data with the ATLAS detector, J. High Energy Phys. 02 (2021) 143.
[35] CMS Collaboration, Search for supersymmetry in proton-proton collisions at 13 TeV in final states with jets and missing transverse momentum, J. High Energy Phys. 10 (2019) 244.
[36] G. Aad *et al.*, Search for chargino-neutralino production with mass splittings near the electroweak scale in three-lepton final states in $\sqrt{s} = 13$ TeV $pp$ collisions with the ATLAS detector, Phys. Rev. D **101**, 072001 (2020).
[37] B. Abi *et al.*, Measurement of the positive muon anomalous magnetic moment to 0.46 ppm, Phys. Rev. Lett. **126**, 141801 (2021).
[38] W. Ahmed, I. Khan, J. Li, T. Li, S. Raza, and W. Zhang, The natural explanation of the muon anomalous magnetic moment via the electroweak supersymmetry from the GmSUGRA in the MSSM, Phys. Lett. B **827**, 136879 (2022).
[39] T. Cheng, J. Li, T. Li, D. V. Nanopoulos, and C. Tong, Electroweak supersymmetry around the electroweak scale, Eur. Phys. J. C **73**, 2322 (2013).
[40] T. Cheng and T. Li, Electroweak Supersymmetry (EWSUSY) in the NMSSM, Phys. Rev. D **88**, 015031 (2013).
[41] T. Li and S. Raza, Electroweak supersymmetry from the generalized minimal supergravity model in the MSSM, Phys. Rev. D **91**, 055016 (2015).
[42] T. Li and D. V. Nanopoulos, Generalizing minimal supergravity, Phys. Lett. B **692**, 121 (2010).
[43] C. Balazs, T. Li, D. V. Nanopoulos, and F. Wang, Supersymmetry breaking scalar masses and trilinear soft terms in generalized minimal supergravity, J. High Energy Phys. 09 (2010) 003.
[44] G. Aad *et al.*, Search for displaced leptons in $\sqrt{s} =$ 13 TeV $pp$ collisions with the ATLAS detector, Phys. Rev. Lett. **127**, 051802 (2021).
[45] G. Aad *et al.*, Search for direct production of charginos, neutralinos and sleptons in final states with two leptons and missing transverse momentum in $pp$ collisions at $\sqrt{s} =$ 8 TeV with the ATLAS detector, J. High Energy Phys. 05 (2014) 071.
[46] G. Aad *et al.*, Searches for electroweak production of supersymmetric particles with compressed mass spectra in $\sqrt{s} = 13$ TeV $pp$ collisions with the ATLAS detector, Phys. Rev. D **101**, 052005 (2020).
[47] S. Carra, Searches for sleptons with the ATLAS detector, Report No. ATL-PHYS-SLIDE-2019-241, 2019.
[48] The ATLAS collaboration, Search for direct pair production of sleptons and charginos decaying to two leptons and neutralinos with mass splittings near the $W$-boson mass in $\sqrt{s} = 13$ TeV $pp$ collisions with the ATLAS detector, J. High Energy Phys. 06 (**2023**) 031.
[49] G. Aad *et al.* (ATLAS Collaboration), Search for electroweak production of charginos and sleptons decaying into final states with two leptons and missing transverse momentum in $\sqrt{s} = 13$ TeV $pp$ collisions using the ATLAS detector, Eur. Phys. J. C **80**, 123 (2020).
[50] S. Ask, A review of the supersymmetry searches at LEP, arXiv:hep-ex/0305007.
[51] A. Heister *et al.*, Search for scalar leptons in $e^+e^-$ collisions at center-of-mass energies up to 209 GeV, Phys. Lett. B **526**, 206 (2002).
[52] The DELPHI Collaboration, Searches for supersymmetric particles in $e^+e^-$ collisions up to 208-GeV and interpretation of the results within the MSSM, Eur. Phys. J. C **31**, 421 (2003).
[53] P. Achard *et al.*, Search for scalar leptons and scalar quarks at LEP, Phys. Lett. B **580**, 37 (2004).
[54] ALEPH, DELPHI, L3, OPAL Experiments, Combined LEP selectron/smuon/stau results, 183–208 GeV, Technical Report No. LEPSUSYWG/04-01.1, CERN, 2004.
[55] W. Ahmed, I. Khan, T. Li, S. Raza, and W. Zhang, Probing relatively heavier right-handed selectron at the CEPC, FCCee and ILC, Phys. Lett. B **832**, 137216 (2022).
[56] N. Aghanim *et al.*, Planck 2018 results. I. Overview and the cosmological legacy of Planck, Astron. Astrophys. **641**, A1 (2020).
[57] M. Dine, A. E. Nelson, and Y. Shirman, Low-energy dynamical supersymmetry breaking simplified, Phys. Rev. D **51**, 1362 (1995).
[58] M. Aaboud *et al.*, Search for long-lived particles produced in $pp$ collisions at $\sqrt{s} = 13$ TeV that decay into displaced hadronic jets in the ATLAS muon spectrometer, Phys. Rev. D **99**, 052005 (2019).
[59] C. Alpigiani *et al.*, An update to the letter of intent for MATHUSLA: Search for long-lived particles at the HL-LHC, arXiv:2009.01693.
[60] L. Lee, C. Ohm, A. Soffer, and T.-T. Yu, Collider searches for long-lived particles beyond the Standard Model, Prog. Part. Nucl. Phys. **106**, 210 (2019); **122**, 103912(E) (2022).
[61] G. Aad *et al.* (ATLAS Collaboration), Search for displaced photons produced in exotic decays of the Higgs boson using 13 TeV $pp$ collisions with the ATLAS detector, Phys. Rev. D **108**, 032016 (2023).
[62] G. Aad *et al.*, Search for nonpointing and delayed photons in the diphoton and missing transverse momentum final state in 8 TeV $pp$ collisions at the LHC using the ATLAS detector, Phys. Rev. D **90**, 112005 (2014).
[63] The ATLAS Collaboration, A detailed map of Higgs boson interactions by the ATLAS experiment ten years after the discovery, Nature (London) **607**, 52 (2022); **612**, E24 (2022).
[64] K. Tamvakis and D. Wyler, Broken global symmetries in supersymmetric theories, Phys. Lett. **112B**, 451 (1982).
[65] K. Rajagopal, M. S. Turner, and F. Wilczek, Cosmological implications of axinos, Nucl. Phys. **B358**, 447 (1991).
[66] T. Goto and M. Yamaguchi, Is axino dark matter possible in supergravity?, Phys. Lett. B **276**, 103 (1992).
[67] E. J. Chun, J. E. Kim, and H. P. Nilles, Axino mass, Phys. Lett. B **287**, 123 (1992).

[68] K.-Y. Choi, L. Covi, J. E. Kim, and L. Roszkowski, Axino cold dark matter revisited, J. High Energy Phys. 04 (2012) 106.

[69] G. Grilli di Cortona, E. Hardy, J. Pardo Vega, and G. Villadoro, The QCD axion, precisely, J. High Energy Phys. 01 (2016) 034.

[70] L. Roszkowski, Axino: New candidate for cold dark matter, in *Proceedings of the 4th International Conference on Particle Physics and the Early Universe* (2001), pp. 71–84.

[71] L. Covi, Axinos as Cold Dark Matter, AIP Conf. Proc. **878**, 145 (2006).

[72] L. Covi, H.-B. Kim, J. E. Kim, and L. Roszkowski, Axinos as dark matter, J. High Energy Phys. 05 (2001) 033.

[73] G. G. Raffelt, Astrophysical axion bounds, Lect. Notes Phys. **741**, 51 (2008).

[74] A. Freitas, F. D. Steffen, N. Tajuddin, and D. Wyler, Late energy injection and cosmological constraints in axino dark matter scenarios, Phys. Lett. B **682**, 193 (2009).

[75] M. Kawasaki, K. Kohri, and T. Moroi, Hadronic decay of late-decaying particles and big-bang nucleosynthesis, Phys. Lett. B **625**, 7 (2005).

[76] K. Jedamzik, Did something decay, evaporate, or annihilate during big bang nucleosynthesis?, Phys. Rev. D **70**, 063524 (2004).

[77] L. Covi, J. E. Kim, and L. Roszkowski, Axinos as cold dark matter, Phys. Rev. Lett. **82**, 4180 (1999).

[78] J. M. No, P. Tunney, and B. Zaldivar, Probing dark matter freeze-in with long-lived particle signatures: MATHUSLA, HL-LHC and FCC-hh, J. High Energy Phys. 03 (2020) 022.

[79] J. Alimena *et al.*, Searching for long-lived particles beyond the Standard Model at the Large Hadron Collider, J. Phys. G **47**, 090501 (2020).

[80] J. Chen, C. Han, J. M. Yang, and M. Zhang, Probing a bino NLSP at lepton colliders, Phys. Rev. D **104**, 015009 (2021).

[81] M. Aaboud *et al.*, Search for supersymmetry in a final state containing two photons and missing transverse momentum in $\sqrt{s} = 13$ TeV $pp$ collisions at the LHC using the ATLAS detector, Eur. Phys. J. C **76**, 517 (2016).

[82] A. Brandenburg, L. Covi, K. Hamaguchi, L. Roszkowski, and F. D. Steffen, Signatures of axinos and gravitinos at colliders, Phys. Lett. B **617**, 99 (2005).

[83] J. R. Ellis, K. Enqvist, D. V. Nanopoulos, and K. Tamvakis, Gaugino masses and grand unification, Phys. Lett. **155B**, 381 (1985).

[84] T. Li, J. A. Maxin, and D. V. Nanopoulos, F-theory grand unification at the colliders, Phys. Lett. B **701**, 321 (2011).

[85] H. Baer, F. E. Paige, S. D. Protopopescu, and X. Tata, ISAJET 7.84: A Monte Carlo event generator for $pp$, $\bar{p}p$, and $e^+e^-$ reactions (1999).

[86] C. Patrignani *et al.*, Review of particle physics, Chin. Phys. C **40**, 100001 (2016).

[87] G. Aad *et al.*, Measurements of the Higgs boson production and decay rates and constraints on its couplings from a combined ATLAS and CMS analysis of the LHC pp collision data at $\sqrt{s} = 7$ and 8 TeV, J. High Energy Phys. 08 (2016) 045.

[88] P. Slavich *et al.*, Higgs-mass predictions in the MSSM and beyond, Eur. Phys. J. C **81**, 450 (2021).

[89] B. C. Allanach, A. Djouadi, J. L. Kneur, W. Porod, and P. Slavich, Precise determination of the neutral Higgs boson masses in the MSSM, J. High Energy Phys. 09 (2004) 044.

[90] CMS and LHCb Collaborations, Observation of the rare $B_s^0 \to \mu^+\mu^-$ decay from the combined analysis of CMS and LHCb data, Nature (London) **522**, 68 (2015).

[91] Y. Amhis *et al.*, Averages of $b$-hadron, $c$-hadron, and $\tau$-lepton properties as of summer 2014, arXiv:1412.7515.

[92] M. Aaboud *et al.*, Search for squarks and gluinos in final states with jets and missing transverse momentum using 36 fb$^{-1}$ of $\sqrt{s} = 13$ TeV $pp$ collision data with the ATLAS detector, Phys. Rev. D **97**, 112001 (2018).

[93] T. A. Vami, Searches for gluinos and squarks, Proc. Sci. LHCP2019 (**2019**) 168.

[94] A. M. Sirunyan *et al.*, Search for new phenomena with the $M_{T2}$ variable in the all-hadronic final state produced in proton–proton collisions at $\sqrt{s} = 13$ TeV, Eur. Phys. J. C **77**, 710 (2017).

[95] G. Aad *et al.*, Search for a scalar partner of the top quark in the all-hadronic $t\bar{t}$ plus missing transverse momentum final state at $\sqrt{s} = 13$ TeV with the ATLAS detector, Eur. Phys. J. C **80**, 737 (2020).

[96] G. Aad *et al.*, Search for new phenomena with top quark pairs in final states with one lepton, jets, and missing transverse momentum in $pp$ collisions at $\sqrt{s} = 13$ TeV with the ATLAS detector, J. High Energy Phys. 04 (2021) 174.

[97] A. M. Sirunyan *et al.*, Search for top squark production in fully-hadronic final states in proton-proton collisions at $\sqrt{s} = 13$ TeV, Phys. Rev. D **104**, 052001 (2021).

[98] A. M. Sirunyan *et al.*, Search for long-lived particles using delayed photons in proton-proton collisions at $\sqrt{s} = 13$ TeV, Phys. Rev. D **100**, 112003 (2019).

[99] D. Curtin *et al.*, Long-lived particles at the energy frontier: The MATHUSLA physics case, Rep. Prog. Phys. **82**, 116201 (2019).

[100] S. Banerjee, B. Bhattacherjee, A. Goudelis, B. Herrmann, D. Sengupta, and R. Sengupta, Determining the lifetime of long-lived particles at the HL-LHC, Eur. Phys. J. C **81**, 172 (2021).

[101] J. Alwall, M. Herquet, F. Maltoni, O. Mattelaer, and T. Stelzer, MadGraph 5: Going beyond, J. High Energy Phys. 06 (2011) 128.

[102] T. Sjöstrand, S. Ask, J. R. Christiansen, R. Corke, N. Desai, P. Ilten, S. Mrenna, S. Prestel, C. O. Rasmussen, and P. Z. Skands, An introduction to PYTHIA 8.2, Comput. Phys. Commun. **191**, 159 (2015).

[103] J. de Favereau, C. Delaere, P. Demin, A. Giammanco, V. Lemaître, A. Mertens, and M. Selvaggi, DELPHES 3, A modular framework for fast simulation of a generic collider experiment, J. High Energy Phys. 02 (2014) 057.